Supplement of Geosci. Model Dev., 19, 2461–2477, 2026
https://doi.org/10.5194/gmd-19-2461-2026-supplement

Geoscientific Model Development
Open Access
EGU

Supplement of

The microbial community model MCoM 1.0: a scalable framework for modelling phototroph–heterotrophic interactions in diverse microbial communities

Leonhard Lücken et al.

Correspondence to: Leonhard Lücken (leonhard.luecken@uol.de)

S1 Parameter reference and notation

Table S1. Parameters of the MCoM model. All parameters are assumed to be non-negative if not stated otherwise.

Parameter	Description	Source code variable	Unit
$V_{N\to i}$	Maximal DIN uptake rates of P_i or H_i	V_NP[i], V_NH[i]	$\mathrm{fmol(N)\,day^{-1}\,cell^{-1}}$
$K_{N\to i}$	Half saturation constants for DIN uptake by P_i or H_i	K_NP[i], K_NH[i]	$\mathrm{mM(N)}$
$V_{j\to i}$	Maximal uptake rates DOC (resp. DON) compound j uptake by H_i	V_DOCH[j,i], V_DONH[j,i]	$\mathrm{fmol(C)\,day^{-1}\,cell^{-1}}$, $\mathrm{fmol(N)\,day^{-1}\,cell^{-1}}$
$K_{j\to i}$	Half saturation constants for DOC (resp. DON) compound j uptake by H_i	K_DOCH[j,i], K_DONH[j,i]	$\mathrm{mM(C)}$, $\mathrm{mM(N)}$
$Y_{j\to i}$	Biomass yield coefficients, i.e., fractions of uptake of DOC (resp. DON) compound D_j integrated into biomass of P_i or H_i, $0 \leq Y_{j\to i} \leq 1$	Y_DOC[j,i], Y_DON[j,i]	-
χ_i^C	Carbon content per cell of population P_i or H_i	XH_C[i], XP_C[i]	$\mathrm{fmol(C)\,cell^{-1}}$
$r_i^{C:N}$, $r_{i\to\mathrm{ex}}^{C:N}$	C:N ratios of populations P_i or H_i, and of N-rich exudates of P_i, $r_i^{C:N} > r_{i\to\mathrm{ex}}^{C:N}$ for all species.	rCN_P[i], rCN_H[i]	$\mathrm{mol(C)\,mol(N)^{-1}}$
$r_i^{\mathrm{Chl}:C}$	Chlorophyll to carbon ratio for cells of P_i	rChlC[i]	$\mathrm{mol(Chl)\,mol(C)^{-1}}$
χ_i^N, χ_i^{Chl}	Nutrient or chlorophyll content per cell ($\chi_i^N = \chi_i^C / r_i^{C:N}$, $\chi_i^{\mathrm{Chl}} = \chi_i^C \cdot r_i^{Chl:C}$)	-	$\mathrm{fmol(N)\,cell^{-1}}$, $\mathrm{fmol(Chl)\,cell^{-1}}$
q_i^{ex}	Maximal fractions of assimilated DOC used for DON exudation of P_i in light limited regime.	q_ex[i]	-
δ_i	Linear loss rates of phytoplankton, heterotrophs, and metabolites	d_P[i], d_H[i], d_M[i]	$\mathrm{day^{-1}}$
$\delta_{q,i}$	Quadratic loss rates of phytoplankton and heterotrophs	d_P2[i]*XP_C[i], d_H2[i]*XH_C[i]	$\mathrm{cell^{-1}\,day^{-1}}$
$a_{j\to i}$	Interaction rate per unit of metabolite j on growth of phytoplankton population i; can be negative	lambda_i *A_MP[j,i]	$\mathrm{day^{-1}}$
$h_{j\to i}$	Half saturation constant for the effect of metabolite j on population i	h_M[j,i]	-
θ_i	Conversion coefficient for determining the amount of metabolite i corresponding to the amount of invested DOC	not included (assumed equal to one)	$\mathrm{mM(C)^{-1}}$
α_i	Slope of the P-I curve of P_i at irradiance $I = 0$. (Effective if variant.use_PI_curve=true)	I_alpha[i]	$\frac{\mathrm{mol(C)\,m^2\,s}}{\mathrm{mol(chl)\,day\,\mu mol(Q)}}$
β_i	Photoinhibition coefficient of the P-I curve of P_i. (Effective if variant.use_PI_curve=true)	I_beta[i]	$\frac{\mathrm{mol(C)\,m^2\,s}}{\mathrm{mol(chl)\,day\,\mu mol(Q)}}$
$\overline{\phi}_i$	Upper limit for the photosynthesis rate of P_i. (Effective if variant.use_PI_curve=true)	I_max[i]	$\mathrm{mol(C)\,mol(Chl)^{-1}\,day^{-1}}$
$\mathrm{R}_{i\to j}$	Release partition coefficients, $0 \leq \mathrm{R}_{i\to j} \leq 1$, for $i \in \mathcal{P}$ or $i \in \mathcal{H}$, and $j \in \mathcal{C}$ or $j \in \mathcal{N}$	R_PDOC[i,j], R_PDON[i,j], R_HDOC[i,j], R_HDON[i,j]	-
$\pi_{i\to j}$	Production of metabolite j by heterotroph H_i	P_HM[i,j]	-
irradiance	Irradiance. If variant.use_PI_curve=false, this is interpreted directly as specific photosynthesis rate with unit $\frac{\mu\mathrm{mol(C)}}{\mu\mathrm{mol(Chl)}\cdot\mathrm{day}}$.	irradiance	$\mathrm{\mu mol(Q)\,m^{-2}\,s^{-1}}$

Table S2. Reference table of notations for elemental flows.

Flow	Description	Source	Target	Unit
	General population-associated flows ($i \in \mathcal{P}$ or $i \in \mathcal{H}$)			
$f_{N\to i}$	realized inorganic nutrient assimilation into biomass	DIN	P_i or H_i	$\mathrm{fmol(N)\,day^{-1}}$
$f^{\max}_{N\to i}$	maximal inorganic nutrient assimilation into biomass	DIN	P_i or H_i	$\mathrm{fmol(N)\,day^{-1}}$
$f_{i\to \mathrm{DOC}}$	total biomass loss to DOC	P_i or H_i	DOC	$\mathrm{fmol(C)\,day^{-1}}$
$f_{i\to \mathrm{DON}}$	total biomass loss to DON	P_i or H_i	DON	$\mathrm{fmol(N)\,day^{-1}}$
	Phytoplankton populations ($i \in \mathcal{P}$)			
$f_{C\to i}$	realized photosynthetic carbon assimilation into biomass	DIC	P_i	$\mathrm{fmol(C)\,day^{-1}}$
$f^{\max}_{C\to i}$	photosynthetic carbon fixation (= maximal assimilation)	DIC	P_i	$\mathrm{fmol(C)\,day^{-1}}$
$f^{i}_{C\to \mathrm{DOC}}$	DOC exudation	DIC	DOC	$\mathrm{fmol(C)\,day^{-1}}$
$f^{i}_{N\to \mathrm{DON}}$	DON exudation	DIN	DON	$\mathrm{fmol(N)\,day^{-1}}$
	Heterotroph populations ($i \in \mathcal{H}$)			
$f_{\mathrm{DOC}\to i}$, $f_{\mathrm{DON}\to i}$	realized total organic carbon, resp. nutrient, assimilation into biomass	DOC, DON	H_i	$\mathrm{fmol(C)\,day^{-1}}$, $\mathrm{fmol(N)\,day^{-1}}$
$f^{\max}_{\mathrm{DOC}\to i}$, $f^{\max}_{\mathrm{DON}\to i}$	maximal total organic carbon, resp. nutrient, assimilation into biomass	DOC, DON	H_i	$\mathrm{fmol(C)\,day^{-1}}$, $\mathrm{fmol(N)\,day^{-1}}$
$f^{\mathrm{up}}_{j\to i}$, $j \in \mathcal{C}\cup\mathcal{N}$	realized uptake of DOC or DON compound j into biomass	D_j	H_i, and DIC or DIN	$\mathrm{fmol(C)\,day^{-1}}$, $\mathrm{fmol(N)\,day^{-1}}$
$f^{\mathrm{up,max}}_{j\to i}$, $j \in \mathcal{C}\cup\mathcal{N}$	maximal uptake of DOC or DON compound j into biomass	D_j	H_i, and DIC or DIN	$\mathrm{fmol(C)\,day^{-1}}$, $\mathrm{fmol(N)\,day^{-1}}$
$f^{i}_{j\to C}$, $f^{i}_{j\to N}$, $j \in \mathcal{C}\cup\mathcal{N}$	remineralization of DOC or DON compound j	D_j	DIC, DIN	$\mathrm{fmol(C)\,day^{-1}}$, $\mathrm{fmol(N)\,day^{-1}}$
$f^{+}_{\mathrm{DON}\to N}$	surplus nutrient remineralization	DON	DIN	$\mathrm{fmol(N)\,day^{-1}}$
	DOC or DON compounds ($j \in \mathcal{C}$ or $j \in \mathcal{N}$)			
$f_{H\to j}$	total heterotroph biomass loss to compound j	H_i	D_j	$\mathrm{fmol(C)\,day^{-1}}$, $\mathrm{fmol(N)\,day^{-1}}$
$f_{P\to j}$	total phototroph biomass loss to compound j	P_i	D_j	$\mathrm{fmol(C)\,day^{-1}}$, $\mathrm{fmol(N)\,day^{-1}}$
$f_{C\to j}$, $f_{N\to j}$	total phototrophic exudation of compound j	DIN, DOC	D_j	$\mathrm{fmol(C)\,day^{-1}}$, $\mathrm{fmol(N)\,day^{-1}}$
$f^{i}_{C\to j}$, $f^{i}_{N\to j}$, $i \in \mathcal{P}$	exudation of compound j by population P_i	DIN, DOC	D_j	$\mathrm{fmol(C)\,day^{-1}}$, $\mathrm{fmol(N)\,day^{-1}}$
$f_{j\to H}$	total assimilation of compound j into heterotroph biomass	D_j	H_i	$\mathrm{fmol(C)\,day^{-1}}$, $\mathrm{fmol(N)\,day^{-1}}$
$f_{j\to C}$, $f_{j\to N}$	total remineralization of compound j	D_j	DIC, DIN	$\mathrm{fmol(C)\,day^{-1}}$, $\mathrm{fmol(N)\,day^{-1}}$
$f_{i\to j}$, $i \in \mathcal{P}\cup\mathcal{H}$	biomass loss of population i to compound j	P_i or H_i	D_j	$\mathrm{fmol(C)\,day^{-1}}$, $\mathrm{fmol(N)\,day^{-1}}$
	Nutrient N			
$f_{\mathrm{DON}\to N}$	total remineralization	DON	DIN	$\mathrm{fmol(N)\,day^{-1}}$
$f_{N\to P}$, $f_{N\to H}$	total assimilation into biomass	DIN	P_i or H_i	$\mathrm{fmol(N)\,day^{-1}}$

S2 Calculation of realized carbon assimilation ($f_{C\to i}$) and DOC exudation rates ($f^i_{C\to\mathrm{DOC}}$)

We use the stoichiometric ratios $r_i^{C:N}$ and $r_{i\to\mathrm{ex}}^{C:N}$, the maximal assimilation rates $f_{C\to i}^{\max}$ and $f_{N\to i}^{\max}$, and the maximal fraction q_i^{ex} of carbon allocated for exudation to derive the realized assimilation and exudation rates $f_{C\to i}$ and $f^i_{C\to\mathrm{DOC}}$.

We assume that carbon is fixated at maximum rate. Since it is fully allocated for assimilation and exudation [Eq. (6) of the main text], we have

$$f_{C\to i} = f_{C\to i}^{\max} - f^i_{C\to\mathrm{DOC}}. \tag{S1}$$

Further, the required uptake of N by P_i, that is $f^i_{N\to\mathrm{DON}} + f_{N\to i}$, is related to the total carbon fixation by the stoichiometric composition of assimilation and exudation fluxes [Eqs. (2) and (7) of the main text]. Dividing these by the ratios, adding them up, then using Eq. (S1) and some basic algebra gives

$$f_{N\to i} + f^i_{N\to\mathrm{DON}} = \frac{r_{i\to\mathrm{ex}}^{C:N}}{r_i^{C:N} r_{i\to\mathrm{ex}}^{C:N}} \cdot f_{C\to i}^{\max} + \frac{r_i^{C:N} - r_{i\to\mathrm{ex}}^{C:N}}{r_i^{C:N} r_{i\to\mathrm{ex}}^{C:N}} \cdot f^i_{C\to\mathrm{DOC}}. \tag{S2}$$

Note that the coefficient of $f^i_{C\to\mathrm{DOC}}$ is positive as we assume $r_i^{C:N} > r_{i\to\mathrm{ex}}^{C:N}$.

This can be solved for $f^i_{C\to\mathrm{DOC}}$ by maximization under the given constraints

$$f^i_{C\to\mathrm{DOC}} \le q_i^{\max} f_{C\to i}^{\max}, \tag{S3}$$

and

$$f_{N\to i} + f^i_{N\to\mathrm{DON}} \le f_{N\to i}^{\max},$$

which, using Eq. (S2), is equivalent to

$$f^i_{C\to\mathrm{DOC}} \le \frac{r_{i\to\mathrm{ex}}^{C:N}}{r_i^{C:N} - r_{i\to\mathrm{ex}}^{C:N}} \left(r_i^{C:N} f_{N\to i}^{\max} - f_{C\to i}^{\max} \right). \tag{S4}$$

Hence,

$$f^i_{C\to\mathrm{DOC}} = \min\left(q_i^{\max} f_{C\to i}^{\max}, \frac{r_{i\to\mathrm{ex}}^{C:N}}{r_i^{C:N} - r_{i\to\mathrm{ex}}^{C:N}} \left(r_i^{C:N} f_{N\to i}^{\max} - f_{C\to i}^{\max} \right) \right).$$

S3 Supplement to Section 3.1

To assess the sensitivity of the mutualistic exchange dynamics in *Synechococcus* co-cultures, we conducted simulations with modified DOC exudation and DON remineralization parameters and compared them to the baseline parametrization used in Section 3.1, cf. Tab. S3. Two perturbed scenarios were tested for each co-culture:

1. Reduced exudation of DOC accessible to heterotrophs ($\mathrm{R}_{P\rightarrow \mathrm{lDOC}} = 0.01$ vs. baseline 0.8 for *R. pomeroyi*, resp. 1.0) for *Tropicibacter*)

2. Reduced DON remineralization (via variant.surplus_remineralization=false and elevated fraction of assimilated DON Y_{DON}: 0.99 vs. 0.75 for *R. pomeroyi*; vs. 0.25 for *Tropicibacter* sp.)

Simulations with reduced DOC exudation [Fig. S1(e,f)] showed diminished heterotroph densities in both co-cultures [Fig. S1(k,l), solid vs. dashed growth curves, e.g., *Tropicibacter* sp. peak: $2.35\times10^9 \rightarrow 1.37\times10^8$ cells mL^{-1} and end density: $5.62\times10^8 \rightarrow 2.80\times10^6$ cells mL^{-1}]. The *Synechococcus* peak density in the *R. pomeroyi* co-culture was slightly higher than for the baseline [$2.32\times10^9 \rightarrow 2.62\times10^9$ cells mL^{-1}; Fig. S1(i), solid vs. dashed growth curves], although final densities decreased ($2.49\times10^7 \rightarrow 1.03\times10^7$ cells mL^{-1}) indicating the stabilizing effect of *R. pomeroyi*. In the *Tropicibacter* co-culture, a reduced exudation has initially positive effects on the *Synechococcus* population as the carbon limitation of *Tropicibacter* reduces the competition for inorganic nutrient [*Syn.* peak density $7.10\times10^8 \rightarrow 1.32\times10^9$ cells mL^{-1}; Fig. S1(j), solid vs. dashed growth curves]. However, there is no recovery of *Synechococcus* in the exudation-restricted scenario.

Reduced DON remineralization severely impairs phototroph viability in simulations [Fig. S1(g,h) and dash-dotted curves in (i,j)]. For this setup, *Synechococcus* densities in both co-cultures collapse quickly after depletion of the inorganic nutrient stock and the recovery in the *Tropicibacter* co-culture is less pronounced. The *Tropicibacter* population closely follows the growth curve of the baseline until $\sim$ day 170 (dash-dotted curve in Fig. S1(l)), but a second growth phase of *Tropicibacter* is prevented by restricted DOC availability due to the reduced *Synechococcus* recovery. This leads to reduced end densities (1.31×10^8 vs. 5.62×10^8 cells mL^{-1} for the baseline). For *R. pomeroyi*, the reduced remineralization allows a growth to significantly higher densities initially, because the fraction of assimilated organic nutrient is increased. In turn, the reduced availability of remineralized nutrient almost halves the peak density of *Synechococcus* to 1.27×10^9 cells mL^{-1} (2.32×10^9 for the baseline). Despite its stronger initial growth, the *R. pomeroyi* density declines faster than for the baseline once the DOC is depleted shortly after day 100 [cf. Fig. S1(g)], leading to a reduced density of 8.65×10^6 cells mL^{-1} at simulation end (1.82×10^7 for the baseline).

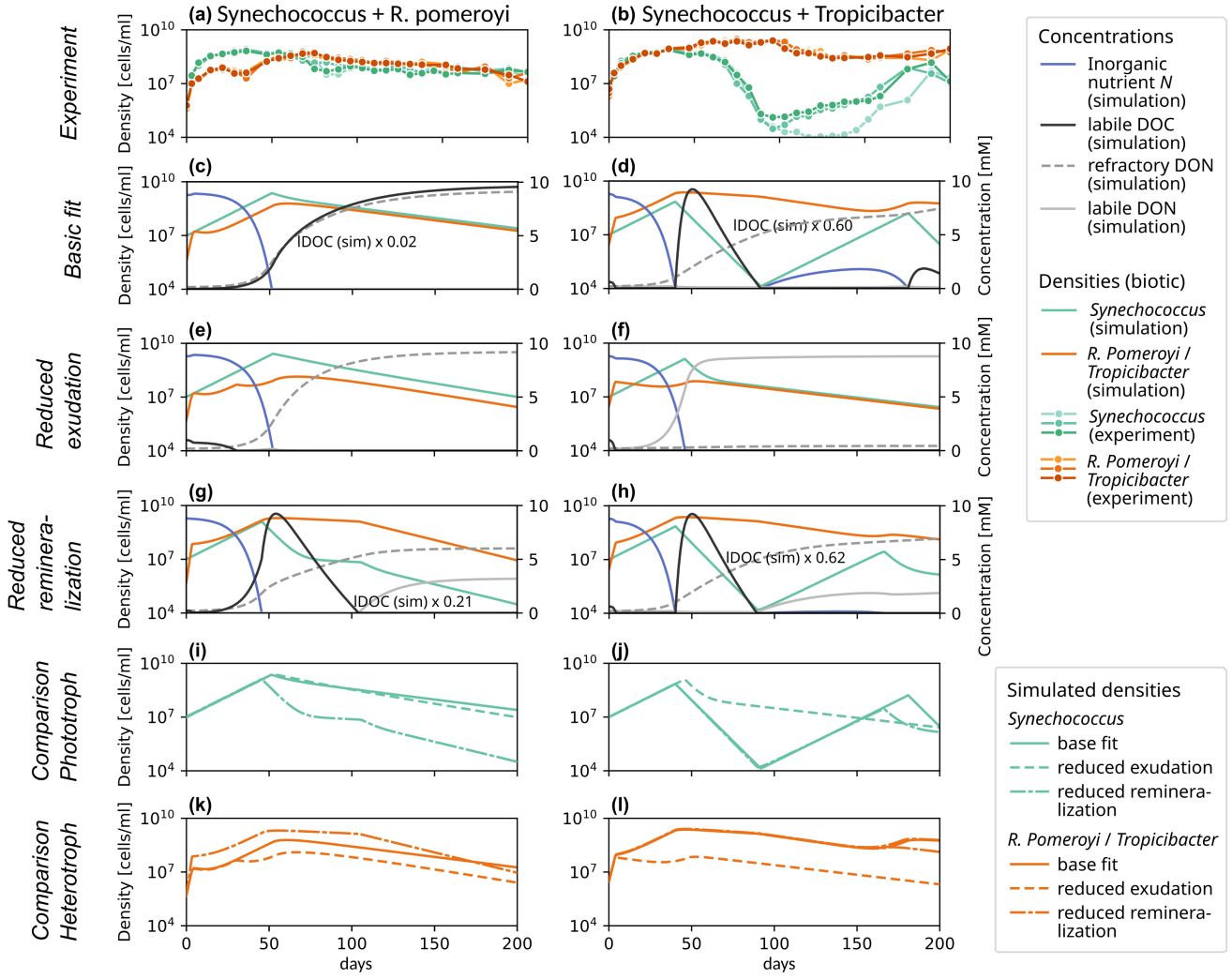

Figure S1. Parameter exploration of Synechococcus experiment modelling (see Section 3.1. Reduced exudation modelled by decreased $R_{P \rightarrow lDOC} = 0.01$, and reduced remineralization by increased $Y_{DON} = 0.99$ and switching off surplus remineralization. Other parameters as in Tab. S3.

Table S3. Parameters for modelling co-culture experiments of *Synechococcus* and heterotrophic bacteria. All parameters were first tuned manually within plausible ranges (cf. Appendix S7). Then, the sum of the R^2-values of the three cultures (axenic, *R. pomeroyi* co-culture, and *Tropicibacter* co-culture) was maximized with respect to parameters V_N, $f_{C\to i}^{\max}$, and δ for *Synechococcus*, and V_{DON}, V_{DOC}, V_{DON}, V_{DON}, and δ for the heterotrophic bacteria.

Parameter	***Synechococcus***	**Parameter**	***R. Pomeroyi***	***Tropicibacter* sp.**
${P_0}^{(1)}$	$10^7\,\mathrm{cells\,mL^{-1}}$	${H_0}^{(1)}$	$5\cdot10^5\,\mathrm{cells\,mL^{-1}}$	$3\cdot10^6\,\mathrm{cells\,mL^{-1}}$
χ^C	$12.0\,\mathrm{fmol(C)\,cell^{-1}}$	χ^C	$12.0\,\mathrm{fmol(C)\,cell^{-1}}$	$12.0\,\mathrm{fmol(C)\,cell^{-1}}$
$r^{C:N}$	$5.2\,\mathrm{mol(C)\,mol(N)^{-1}}$	$r^{C:N}$	$4.0\,\mathrm{mol(C)\,mol(N)^{-1}}$	$4.0\,\mathrm{mol(C)\,mol(N)^{-1}}$
${f_{C\to i}^{\max}}^{(*,2)}$	$7.778\,\mathrm{fmol(C)\,day^{-1}\,cell^{-1}}$	$\delta^{(*)}$, δ_q	$0.217\,\mathrm{day^{-1}}$, $0.0\,(10^6\,\mathrm{cells})^{-1}\,\mathrm{day^{-1}}$	$0.2\,\mathrm{day^{-1}}$, $0.0\,(10^6\,\mathrm{cells})^{-1}\,\mathrm{day^{-1}}$
$\delta^{(*)}$, δ_q	$0.217\,\mathrm{day^{-1}}$, $0.0\,(10^6\,\mathrm{cells})^{-1}\,\mathrm{day^{-1}}$	${V_N}^{(3)}$	$0.0\,\mathrm{fmol(N)\,cell^{-1}\,day^{-1}}$	$4.0\,\mathrm{fmol(N)\,cell^{-1}\,day^{-1}}$
${V_N}^{(*)}$	$0.746\,\mathrm{fmol(N)\,cell^{-1}\,day^{-1}}$	${K_N}^{(3)}$	-	$1.0\,\mu\mathrm{M(N)}$
K_N	$2.0\,\mu\mathrm{M(N)}$	${V_{DON}}^{(*)}$	$19.80\,\mathrm{fmol(N)\,cell^{-1}\,day^{-1}}$	$1.074\,\mathrm{fmol(N)\,cell^{-1}\,day^{-1}}$
		K_{DON}	$0.1\,\mathrm{mM(N)}$	$0.1\,\mathrm{mM(N)}$
	Environment	${Y_{DON}}^{(*)}$	0.254	0.754
${N_0}^{(1)}$	$8.8\,\mathrm{mM(N)}$	${V_{DOC}}^{(*)}$	$23.65\,\mathrm{fmol(N)\,cell^{-1}\,day^{-1}}$	$16.59\,\mathrm{fmol(N)\,cell^{-1}\,day^{-1}}$
Δ	$0.0\,\mathrm{day^{-1}}$	K_{DOC}	$0.1\,\mathrm{mM(C)}$	$0.1\,\mathrm{mM(C)}$
		${Y_{DOC}}^{(*)}$	0.865	0.850
		$\mathrm{R}_{H\to\mathrm{lDOC}}$	0.5	0.99
		$\mathrm{R}_{P\to\mathrm{lDOC}}$	0.8	1.0
		$\mathrm{R}_{H\to\mathrm{lDON}}$	0.9	0.93
		$\mathrm{R}_{P\to\mathrm{lDON}}$	0.8	1.0

$^{(*)}$ Parameter value from optimization.

$^{(1)}$ Chosen according to Christie-Oleza et al. (2017).

$^{(2)}$ Constant photosynthetic rate.

$^{(3)}$ *R. pomeroyi* did not use the supplied NH_4 (Christie-Oleza et al., 2017).

S4 Supplement to Section 3.2

Figure S2 illustrates the sensitivity of *Prochlorococcus* growth curves to variations in key heterotroph parameters under promoting [Panels (a–g)], neutral [interaction rate $a_M = 0.0$; Panels (h–n)] and inhibiting [Panels (o–u)] co-culture simulations. Note that the neutral case differs from the axenic configuration, where no heterotrophs are present; instead, metabolites produced do not affect the phototroph. The growth curves for the base parameters are shown in red and the simulated axenic growth curve is shown using a dashed grey line for reference. Panels (a,h,o) show the same transition from the promoting to the inhibitory scenario through variation of the metabolite interaction rate ($a_M : -0.137 \rightarrow 0.114\ \mathrm{day}^{-1}$). This illustrates the non-linear effect of interactions on peak height and timing, which is in line with the effects found in experiments by Sher et al. (2011). Panels (b,i,p) show that higher heterotroph loss rates (δ) result in higher phototroph peak densities in all scenarios. This is a consequence of the reduced competition for nutrient between phototrophs and heterotrophs. The maximal heterotrophic nutrient uptake rate (V_N) likewise influences heterotroph competitive ability for the limiting nutrient, leading to similar patterns in Panels (c,j,k). Variations in maximal heterotrophic uptake rates for DOC and DON [V_{DOC} and V_{DON}, Panels (d,k,r) and (e,l,s)], affect phototroph growth when heterotrophs are limited. This is the case for $V_{DON} \lesssim 1.5$ and for $V_{DOC} \lesssim 3.0$. For V_{DOC} the effect is not always linear as increased heterotroph presence can benefit *Prochlorococcus* if elevated nutrient remineralization compensates for nutrient competition. In every scenario, severe heterotroph limitation approximates the axenic growth curve. Variation of the DOC yield coefficient Y_{DOC} [Panels (f,m,t)] exhibits similar effects as V_{DOC} for growth limiting values. However, the tested range ($Y_{DOC} \in [0.3, 1.0]$) does not lead to significant effects in the growth promoting scenario. The DON-Yield coefficient Y_{DON} [Panels (g,n,u)] has complex effects, controlling both heterotroph growth rate and DON remineralization, in some cases inducing a second growth phase for the phototrophs.

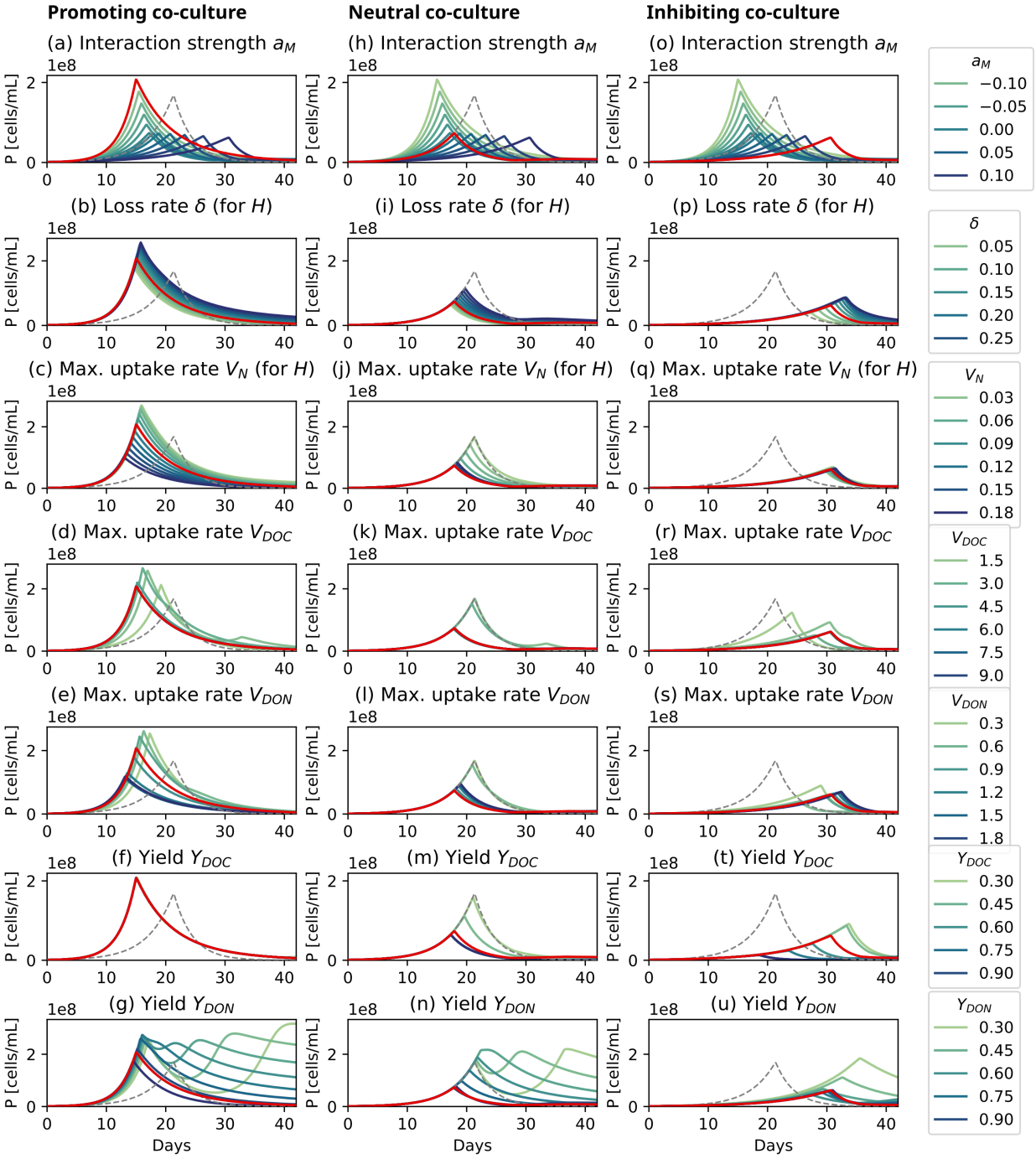

Figure S2. Sensitivity analysis for *Prochlorococcus* modelling (see Section 3.2). Left column (a–g): Promoting co-culture; Middle column (h–n): Neutral co-culture ($a_M = 0$); Right column (o–u): Inhibiting interactions. Red curves show the simulated *Prochlorococcus* growth curves for parameters corresponding to the base fit (see Table S4) and the dashed grey curve shows the axenic growth curve.

Table S4. Parameters for modelling Co-culture experiments of *Prochlorococcus* and heterotrophic bacteria. All parameters were first tuned manually within plausible ranges (cf. Appendix S7). Then, the total root mean square error (RMSE) of the simulation results for axenic, promoting and inhibiting cases was minimized with respect to parameters V_N and δ_P for *Prochlorococcus*, V_{DOC}, Y_{DOC} (same value for both heterotrophs) and a_M for the positive and negative interaction. Additionally, we assumed a linear conversion of relative fluorescence units (RFU) to cell numbers for *Prochlorococcus* and subjected the scaling factor to the optimization yielding $42,402\,\mathrm{cells\,RFU^{-1}}$.

	Prochlorococcus		**Heterotrophs**
$P_0{}^{(1)}$	$10^6\,\mathrm{cells\,mL^{-1}}$	H_0	$10^4\,\mathrm{cells\,mL^{-1}}$
χ_C	$10.0\,\mathrm{fmol(C)\,cell^{-1}}$	χ_C	$2.0\,\mathrm{fmol(C)\,cell^{-1}}$
$r_i^{C:N}$	$5.0\,\mathrm{mol(C)\,mol(N)^{-1}}$	$r_i^{C:N}$	$4.0\,\mathrm{mol(C)\,mol(N)^{-1}}$
$f_{C\to i}^{\max}$	$10.0\,\mathrm{fmol(C)\,day^{-1}\,cell^{-1}}$ (constant photosynthetic rate)	δ, δ_q	$0.1\,\mathrm{day^{-1}}$, $0.0\,(10^6\,\mathrm{cells})^{-1}\,\mathrm{day^{-1}}$
$\delta^{(*)}$, δ_q	$0.324\,\mathrm{day^{-1}}$, $0.0\,\mathrm{cell^{-1}}\,(10^6\,\mathrm{cells})^{-1}\,\mathrm{day^{-1}}$	V_N	$0.9\,\mathrm{fmol(N)\,cell^{-1}\,day^{-1}}$
V_N	$1.135\,\mathrm{fmol(N)\,cell^{-1}\,day^{-1}}$	K_N	$8.0\,\mu\mathrm{M(N)}$
K_N	$2.4\,\mu\mathrm{M}$	V_{DON}	$3.0\,\mathrm{fmol(N)\,cell^{-1}\,day^{-1}}$
		K_{DON}	$0.6\,\mathrm{mM(N)}$
	Environment	$Y_{DON}{}^{(*)}$	0.927
$N_0{}^{(1)}$	$0.8\,\mathrm{mM(N)}$	$V_{DOC}{}^{(*)}$	$6.94\,\mathrm{fmol(N)\,cell^{-1}\,day^{-1}}$
Δ	$0.0\,\mathrm{day^{-1}}$	K_{DOC}	$0.6\,\mathrm{mM(C)}$
$l\mathrm{DOC}_0{}^{(1)}$	$5.0\,\mathrm{mM(C)}$	Y_{DOC}	0.5
$l\mathrm{DON}_0{}^{(1)}$	$0.5\,\mathrm{mM(N)}$	h_M	10^{-8}
M_0	10^{-9}/L	π_M	10^{-7}
δ_M	$0.3\,\mathrm{day^{-1}}$		
	Rhodobacterales **(HOT5B8)**		***Marinobacter*** **(HOT4B5)**
$a_M{}^{(*)}$	-0.137	$a_M{}^{(*)}$	0.114

$^{(*)}$ Parameter value from optimization.

$^{(1)}$ Chosen according to Sher et al. (2011).

S5 Supplement to Section 3.3

We assessed the robustness of the periodic regime (Section 3.3) against the variation of two parameters. Figure S3 reports a parameter scan with varying maximal specific nutrient uptake rate $V_{N\to1}$ of phytoplankton species P_1. Panel (a) shows how average phytoplankton densities vary with $V_{N\to1}$, where the dashed line indicates P_1's fluctuation amplitude $\mathrm{amp}(P_1) = \max(P_1) - \min(P_1)$. Zero amplitude values (for $V_{N\to1} \leq 0.25$) correspond to stable equilibria, where P_1 goes extinct, leading P_2 to displace P_3 through superior nutrient affinity ($V_{N\to2} > V_{N\to3}$). For $V_{N\to1} \in [0.65, 1.65]$, variants of the cyclic dominance pattern reported in Fig. 6 of the main text persist with consistent amplitudes and average densities, though above $V_{N\to1} = 1.2$, single peaks evolve into multi-peak bursts (particularly evident in P3 and H3; Panels (d–f)), with burst complexity increasing stepwise to ≥ 4 peaks at $V_{N\to1} = 1.85$ (Panel f). The transition region ($V_{N\to1} \in [0.35, 0.65]$) exhibits irregular fluctuations (Panels b–c). At higher values ($V_{N\to1} \geq 1.85$), we observe an abrupt amplitude reduction accompanied by a sharp P1 density increase that represses other populations amid moderate fluctuations (Panel g). The scan employed continuation methods to track stable regimes: starting into negative and positive direction from Section 3.3's parameter value (vertical dashed line), each subsequent simulation was initialized from the previous simulation's final state.

Periodic fluctuations are dependent on interaction strength, as well. Figure S4(a) presents a parameter scan over the interaction rates $a_{i\to i+1}$ (note that these are identical). Beginning the continuation at $a_{i\to i+1} = -1.0$, we observe sustained cyclic dominance regimes throughout $a_{i\to i+1} \in [-1.0, -0.55]$, with slightly shorter oscillation periods for weaker interaction strength (Panels b–d). Average population densities are nearly identical for the three phytoplankton species. This solution branch is lost at $a_{i\to i+1} = -0.55$, revealing a branch of equilibria with initially substantially different densities for the different species ($a_{i\to i+1} \in [-0.55, -0.35]$), but then converging to similar values for $a_{i\to i+1} \in [-0.35, 0.0]$.

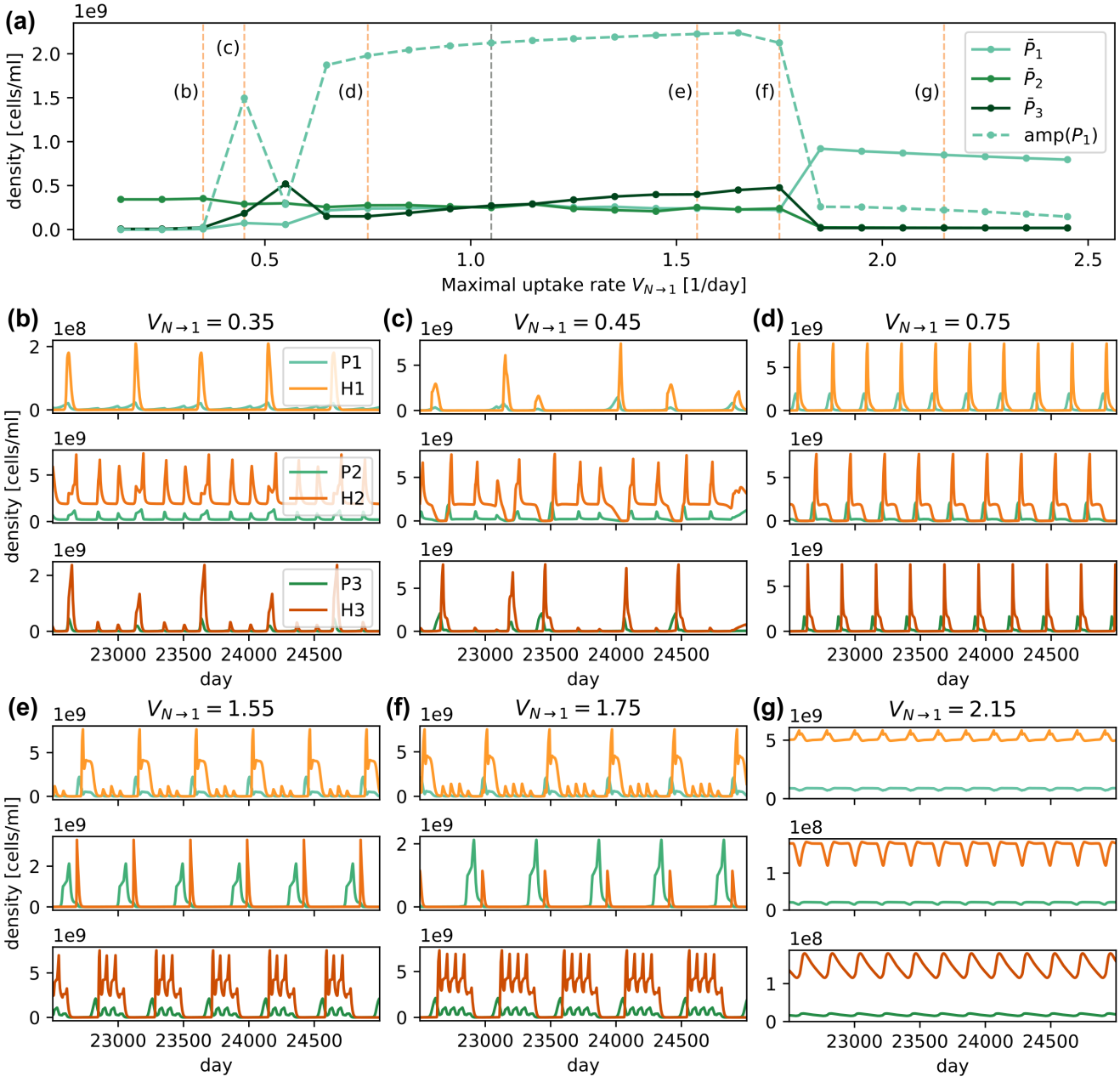

Figure S3. Robustness of cyclic dominance to $V_{N\to1}$ variation. (a) Average phytoplankton densities (solid green lines) and P_1 fluctuation amplitude (dashed green curve) versus maximal uptake rate $V_{N\to1}$. (b–g) Time series at representative $V_{N\to1}$ values showing: (b,c) irregular fluctuations; (d) cyclic dominance; (e,f) multi-peak bursts; and (g) P_1-dominant regime. Parameters other than $V_{N\to1}$ as in Tab. S5.

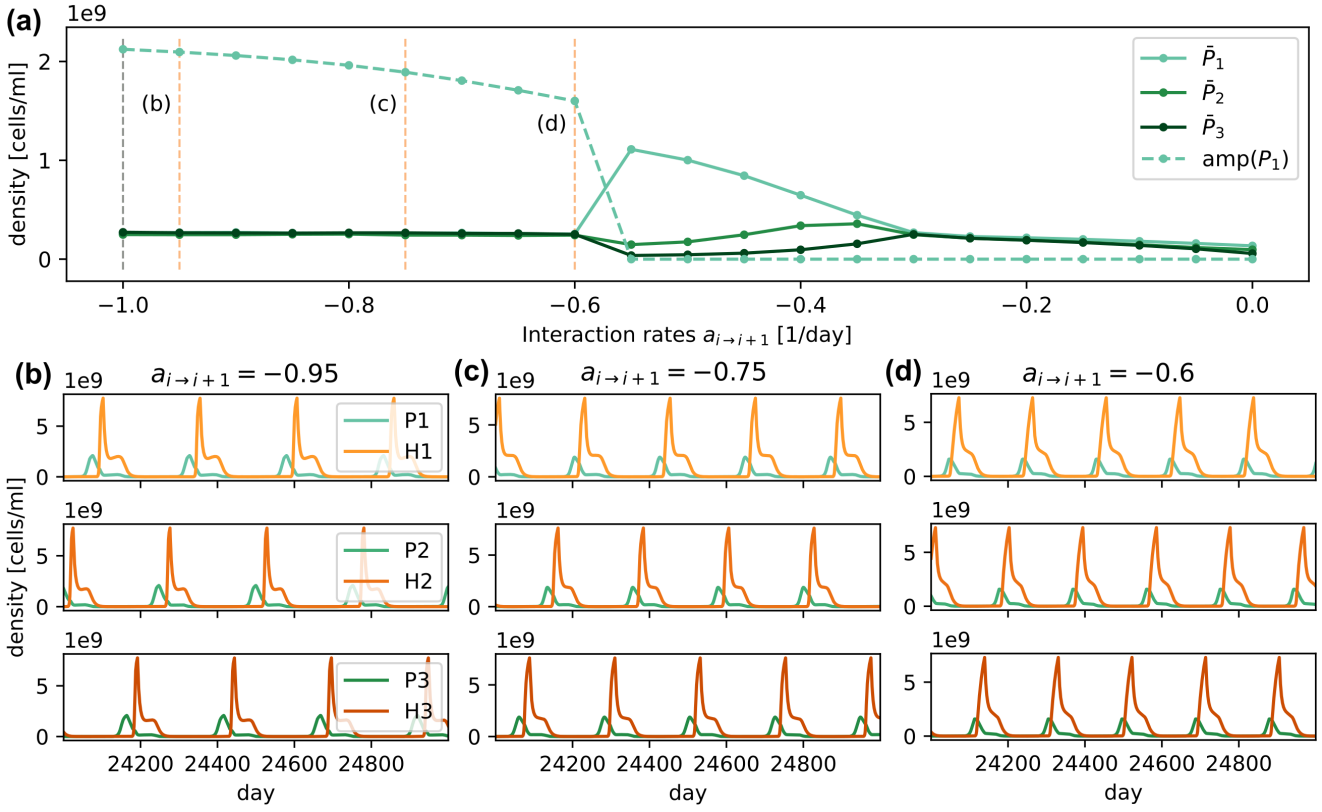

Figure S4. Robustness of cyclic dominance to interaction strength variation. (a) Average phytoplankton densities (solid green lines) and P_1 fluctuation amplitude (dashed green curve) versus interaction rates $a_{i\to i+1}$. (b–d) Time series at representative $a_{i\to i+1}$ values. Parameters other than $a_{i\to i+1}$ as in Tab. S5.

Table S5. Parameters used for the cyclic interaction motif, see Sec. 3.3.

Parameter	**Phytoplankton**	**Parameter**	**Heterotrophs**
χ_i^C	$10.0\,\mathrm{fmol(C)\,cell^{-1}}$	χ_i^C	$2.0\,\mathrm{fmol(C)\,cell^{-1}}$
$r_i^{C:N}$	$5.2\,\mathrm{mol(C)\,mol(N)^{-1}}$	$r_i^{C:N}$	$4.0\,\mathrm{mol(C)\,mol(N)^{-1}}$
δ_i, $\delta_{q,i}$	$0.2\,\mathrm{day^{-1}}$, $0.2\,(10^6\,\mathrm{cells})^{-1}\,\mathrm{day^{-1}}$	δ_i, $\delta_{q,i}$	$0.1\,\mathrm{day^{-1}}$, $0.02\,(10^6\,\mathrm{cells})^{-1}\,\mathrm{day^{-1}}$
$h_{j\to i}$	10^{-4}	$\pi_{i\to j}$	10^{-5}
$a_{j\to i}$	0.0 or -1.0 for $i=j+1$	**Nutrient uptake**	
$V_{N\to i}$	$1.0\,\mathrm{fmol(N)\,cell^{-1}\,day^{-1}}$	$V_{N\to i}$	$1.5\,\mathrm{fmol(N)\,cell^{-1}\,day^{-1}}$
$K_{N\to i}$	$2.0\,\mu\mathrm{M(N)}$	$K_{N\to i}$	$8.0\,\mu\mathrm{M(N)}$
$\overline{\phi}_i$	$5.0\,\mathrm{mol(C)\,mol(Chl)^{-1}\,day^{-1}}$	**DON uptake**	
α_i	$0.08\ \frac{\mathrm{mol(C)\,m^2\,s}}{\mathrm{mol(chl)\,day\,\mu mol(Q)}}$	$V_{j\to i}$	$3.0\,\mathrm{fmol(N)\,cell^{-1}\,day^{-1}}$
β_i	$0.003\ \frac{\mathrm{mol(C)\,m^2\,s}}{\mathrm{mol(chl)\,day\,\mu mol(Q)}}$	$K_{j\to i}$	$1.0\,\mu\mathrm{M(N)}$
		$Y_{j\to i}$	0.5
Environment		**DOC uptake**	
Δ	$0.1\,\mathrm{day^{-1}}$	$V_{j\to i}$	$4.0\,\mathrm{fmol(N)\,cell^{-1}\,day^{-1}}$
δ_M	$0.1\,\mathrm{day^{-1}}$	$K_{j\to i}$	$1.0\,\mu\mathrm{M(C)}$
N_{ext}	$5.0\,\mu\mathrm{M(N)}$	$Y_{j\to i}$	0.5
I	$10.0\,\mu\mathrm{mol(Q)\,m^{-2}\,day^{-1}}$		

S6 Supplement for Section 3.4

Table S6. Parameters used for the simulation of two competing consortia, see Sec. 3.4

Parameter	**Phytoplankton**	**Parameter**	**Heterotrophs**
$P_i\,(0)$	10^8, resp. 10^6, cells mL^{-1}	$H_i\,(0)$	10^5–10^7 cells mL^{-1}
χ_i^C	10.0 fmol(C) cell^{-1}	χ_i^C	2.0 fmol(C) cell^{-1}
$r_i^{C:N}$	5.2 mol(C) $\mathrm{mol(N)}^{-1}$	$r_i^{C:N}$	4.0 mol(C) $\mathrm{mol(N)}^{-1}$
δ_i, $\delta_{q,i}$	0.1 day^{-1}, 1.0 $(10^6\ \mathrm{cells})^{-1}\,\mathrm{day}^{-1}$	δ_i, $\delta_{q,i}$	0.1 day^{-1}, 0.02 $(10^6\ \mathrm{cells})^{-1}\,\mathrm{day}^{-1}$
$h_{j\to i}$	10^{-4}	$\pi_{i\to j}$	10^{-5}
$a_{j\to i}$	0.0 or -0.1	**Nutrient uptake**	
$V_{N\to i}$	1.0 fmol(N) $\mathrm{cell}^{-1}\,\mathrm{day}^{-1}$	$V_{N\to i}$	1.5 fmol(N) $\mathrm{cell}^{-1}\,\mathrm{day}^{-1}$
$K_{N\to i}$	2.0 mM(N)	$K_{N\to i}$	8.0 mM(N)
$\overline{\phi}_i$	3.0–5.0 mol(C) $\mathrm{mol(Chl)}^{-1}\,\mathrm{day}^{-1}$	**DON uptake**	
α_i	0.05–0.3 $\frac{\mathrm{mol(C)\,m^2\,s}}{\mathrm{mol(chl)\,day\,\mu mol(Q)}}$	$V_{j\to i}$	3.0 fmol(N) $\mathrm{cell}^{-1}\,\mathrm{day}^{-1}$
β_i	0.003–0.08 $\frac{\mathrm{mol(C)\,m^2\,s}}{\mathrm{mol(chl)\,day\,\mu mol(Q)}}$	$K_{j\to i}$	1.0 mM(N)
		$Y_{j\to i}$	0.5
Environment		**DOC uptake**	
Δ	0.1 day^{-1}	$V_{j\to i}$	4.0 fmol(N) $\mathrm{cell}^{-1}\,\mathrm{day}^{-1}$
N_0	8.8 mM(N)	$K_{j\to i}$	1.0 mM(C)
δ_M	0.1 day^{-1}	$Y_{j\to i}$	0.5
N_{ext}	5.0 mM(N)		
$I_{\min}$	0.0 µmol(Q) $\mathrm{m}^{-2}\,\mathrm{day}^{-1}$	**Connectivity**	
$I_{\max}$	125.0 µmol(Q) $\mathrm{m}^{-2}\,\mathrm{day}^{-1}$	exPDOC	4
		exPDON	4
System dimensions		exHDOC	4
dims.P	20	exHDON	4
dims.H	20	upDOCH	3
dims.DOC	20	upDONH	3
dims.DON	20	prodHM	2
dims.M	10–20 (overlap-depd.)	effsMP	4

S7 Empirical parameter constraints

To provide an orientation for parameter selection, we present a concise literature survey of typical value ranges for model components. While offering practical guidance, this compilation is not exhaustive; parameters should be adapted to specific research contexts. Note that we reproduce the values in units given in the original source, as conversions may involve further assumptions. Where these units deviate from model units we provide conversion factors.

S7.1 Stoichiometry parameters

Phototrophic, as well as heterotrophic, cellular elemental composition varies substantially due to taxonomic differences, nutrient availability, and environmental conditions. For instance, cyanobacterial carbon content varies over 20-fold (0.83–20.33 $\mathrm{fmol(C)\,cell^{-1}}$; Tab. S7), and C:N ratios range from 4 to 23 $\mathrm{mol(C)\,mol(N)^{-1}}$ (Tab. S8), and heterotrophic bacteria show carbon content spanning more than two orders of magnitude (0.49–143 $\mathrm{fmol(C)\,cell^{-1}}$; Tab. S9) and highly flexible C:N ratios (2.3–12.0 $\mathrm{mol(C)\,mol(N)^{-1}}$; Tab. S10). Cell sizes and, correspondingly, cellular carbon content of eukaryotic algae varies even stronger depending on taxon and growth conditions. Thus, parameter selection should account for the modelled environment and physiological state. Most data in Tables S7–S10 originate from laboratory cultures or specific environments; natural communities may exhibit broader ranges due to taxonomic diversity and environmental gradients.

Table S7. Reported ranges for phytoplankton cellular carbon content (χ_P^C).

Range	**Unit**	**Conversion to model unit** $(\mathrm{fmol(C)\,cell^{-1}})$	**Note**	**Source**
~10–70	$\mathrm{fg(C)\,cell^{-1}}$	$\frac{\mathrm{fmol(C)}}{12\,\mathrm{fg(C)}}$	*Prochlorococcus*	Grob et al. (2013)
~50–95	$\mathrm{fg(C)\,cell^{-1}}$	$\frac{\mathrm{fmol(C)}}{12\,\mathrm{fg(C)}}$	*Synechococcus*	Grob et al. (2013)
46–61	$\mathrm{fg(C)\,cell^{-1}}$	$\frac{\mathrm{fmol(C)}}{12\,\mathrm{fg(C)}}$	*Prochlorococcus* MED4	Bertilsson et al. (2003)
17–124	$\mathrm{fg(C)\,cell^{-1}}$	$\frac{\mathrm{fmol(C)}}{12\,\mathrm{fg(C)}}$	*Prochlorococcus*, literature overview	Bertilsson et al. (2003)
92–132	$\mathrm{fg(C)\,cell^{-1}}$	$\frac{\mathrm{fmol(C)}}{12\,\mathrm{fg(C)}}$	*Synechococcus* WH8012	Bertilsson et al. (2003)
213–244	$\mathrm{fg(C)\,cell^{-1}}$	$\frac{\mathrm{fmol(C)}}{12\,\mathrm{fg(C)}}$	*Synechococcus* WH8103	Bertilsson et al. (2003)
27–5.87×10^3	$\mathrm{pg(C)\,cell^{-1}}$	$\frac{10^3\,\mathrm{fmol(C)}}{12\,\mathrm{pg(C)}}$	Diatoms	Tas (2023)
2.06×10^2–4.84×10^4	$\mathrm{pg(C)\,cell^{-1}}$	$\frac{10^3\,\mathrm{fmol(C)}}{12\,\mathrm{pg(C)}}$	Dinoflagellates	Tas (2023)

Table S8. Reported ranges for phytoplankton carbon-to-nitrogen ratio ($r_P^{C:N}$).

Range	Unit	Note	Source
4.4–10.0	$\mathrm{mol(C)\ mol(N)^{-1}}$	*Synechococcus* (strains)	Bertilsson et al. (2003)
5.7–9.9	$\mathrm{mol(C)\ mol(N)^{-1}}$	*Prochlorococcus*	Bertilsson et al. (2003)
4.57–7.28	$\mathrm{mol(C)\ mol(N)^{-1}}$	*Prochlorococcus*/*Synechococcus* (North Atlantic, surface)	Grob et al. (2013)
4.41–5.83	$\mathrm{mol(C)\ mol(N)^{-1}}$	*Prochlorococcus*/*Synechococcus* (North Atlantic, deep)	Grob et al. (2013)
4–17 (avg. 7.7)	$\mathrm{mol(C)\ mol(N)^{-1}}$	Eukaryotic phytoplankton	Bertilsson et al. (2003)
6.625	$\mathrm{mol(C)\ mol(N)^{-1}}$	Redfield ratio	Redfield (1958)
6.8–7.8	$\mathrm{mol(C)\ mol(N)^{-1}}$	marine POC (95% CI)	Geider and La Roche (2002)
5.1–8.5	$\mathrm{mol(C)\ mol(N)^{-1}}$	Green algae	Finkel et al. (2016)
5.2–8.4	$\mathrm{mol(C)\ mol(N)^{-1}}$	Haptophytes	Finkel et al. (2016)
5.1–13.3	$\mathrm{mol(C)\ mol(N)^{-1}}$	Diatoms	Finkel et al. (2016)
5.0–11.3	$\mathrm{mol(C)\ mol(N)^{-1}}$	Dinoflagellates	Finkel et al. (2016)
6.8–8.7	$\mathrm{mol(C)\ mol(N)^{-1}}$	Nutrient-replete phytoplankton (95% CI)	Geider and La Roche (2002)
7–20	$\mathrm{mol(C)\ mol(N)^{-1}}$	Marine eukaryotes under N starvation	Goldman et al. (1979)

Table S9. Reported ranges for heterotrophic bacterial cellular carbon content (χ_H^C).

Range	Unit	Conversion to model unit ($\mathrm{fmol(C)\ cell^{-1}}$)	Note	Source
1.04–143	$\mathrm{fmol(C)\ cell^{-1}}$	–	Freshwater isolates (24 strains)	Godwin and Cotner (2015)
5.9–23.5 (mean: 12.4)	$\mathrm{fg(C)\ cell^{-1}}$	$\times 1/12\ \mathrm{fmol(C)/fg(C)}$	Oceanic assemblages	Fukuda et al. (1998)
15.7–47.9 (mean: 30.2)	$\mathrm{fg(C)\ cell^{-1}}$	$\times 1/12\ \mathrm{fmol(C)/fg(C)}$	Estuarine/coastal assemblages	Fukuda et al. (1998)
88–106 (means)	$\mathrm{fg(C)\ cell^{-1}}$	$\times 1/12\ \mathrm{fmol(C)/fg(C)}$	Nutrient-limited marine bacteria	Vrede et al. (2002)
32–50 (means)	$\mathrm{fg(C)\ cell^{-1}}$	$\times 1/12\ \mathrm{fmol(C)/fg(C)}$	C-limited marine bacteria	Vrede et al. (2002)
128–156 (means)	$\mathrm{fg(C)\ cell^{-1}}$	$\times 1/12\ \mathrm{fmol(C)/fg(C)}$	Replete marine cultures	Vrede et al. (2002)

Table S10. Reported ranges for heterotrophic molar carbon-to-nitrogen ratio ($r_H^{C:N}$).

Range	Unit	Note	Source
3.6–4.0	$\mathrm{mol(C)\ mol(N)^{-1}}$	Marine bacteria	Fagerbakke et al. (1996)
5.0–5.9	$\mathrm{mol(C)\ mol(N)^{-1}}$	Freshwater bacteria	Fagerbakke et al. (1996)
2.3–11.0 (median 5.06)	$\mathrm{mol(C)\ mol(N)^{-1}}$	Freshwater isolates	Godwin and Cotner (2015)
4.9–12.0 (means)	$\mathrm{mol(C)\ mol(N)^{-1}}$	Nutrient-limited marine bacteria	Vrede et al. (2002)
3.6–4.1 (means)	$\mathrm{mol(C)\ mol(N)^{-1}}$	C-limited marine bacteria	Vrede et al. (2002)
3.8–6.3 (means)	$\mathrm{mol(C)\ mol(N)^{-1}}$	Replete marine cultures	Vrede et al. (2002)
5.4–8.3 (mean: 6.8)	$\mathrm{mol(C)\ mol(N)^{-1}}$	Oceanic assemblages	Fukuda et al. (1998)
5.0–7.7 (mean: 5.9)	$\mathrm{mol(C)\ mol(N)^{-1}}$	Estuarine/coastal assemblages	Fukuda et al. (1998)
5.3–6.2	$\mathrm{mol(C)\ mol(N)^{-1}}$	Marine cultures (Gulf of Mexico)	Kroer et al. (1994)
8.0–8.8	$\mathrm{mol(C)\ mol(N)^{-1}}$	Estuarine cultures	Kroer et al. (1994)
5.2–7.5	$\mathrm{mol(C)\ mol(N)^{-1}}$	Eutrophic riverine cultures	Kroer et al. (1994)

S7.2 Inorganic Nutrient Uptake Parameters

Resource uptake in MCoM is modelled through Michaelis-Menten kinetics, characterized by maximal uptake rates and half-saturation constants (V_N and K_N for inorganic nutrient). These parameters vary substantially with nutrient species, environmental conditions, and organism groups (Tables S11, S12).

For heterotrophic bacteria, direct quantitative parameter values are limited; however, comparative studies indicate higher growth rates of phytoplankton in replete environments ($V_{N\to H} < V_{N\to P}$, while, due to smaller bacterial cell sizes, bacteria generally exhibit higher affinities ($V_{N\to H}/K_{N\to H} > V_{N\to H}/K_{N\to P}$), conferring an overall advantage at low nutrient concentrations (Kirchman, 1994). Metabolic adaptation may lead to lower half-saturation constants K_N in oligotrophic environments than in eutrophic within the same species (Kovarova and Egli, 1998). Uptake rates also vary by nitrogen species, with NH_4^+ uptake typically exceeding NO_3^- uptake. Note that MCoM currently does not account for these separately; the maximal uptake rate V_N represents total DIN uptake.

Converting uptake rates to model units ($\mathrm{fmol(N)\,cell^{-1}\,day^{-1}}$) requires caution due to dependencies on cellular stoichiometry and size. For instance, to convert specific uptake rates in $\mathrm{h^{-1}}$ (nitrogen uptake normalized by biomass nitrogen), values should be multiplied by cellular nitrogen content ($\chi^N = \chi^C / r^{C:N}$) and by 24 to obtain daily rates; and, for rates in $\mathrm{mol(NO_3)\,(mol(C)\,day)^{-1}}$, by cellular carbon content (χ^C, $\mathrm{fmol(C)\,cell^{-1}}$).

Table S11. Specific DIN uptake rates V_N for phytoplankton and heterotrophic bacteria .

Range	Unit	Conversion to model unit $(\mathrm{fmol(N)\,(cell\,day)^{-1}})$	Note	Source
~0.12	$\mathrm{h^{-1}}$	$(24 \cdot \chi^C / r^{C:N})$ h $\mathrm{day^{-1}}$	*Phaeocystis* colonies (>35 µm, NH_4)	Bradley et al. (2010)
~0.013	$\mathrm{h^{-1}}$	$(24 \cdot \chi^C / r^{C:N})$ h $\mathrm{day^{-1}}$	*Phaeocystis* colonies (>35 µm, NO_3)	Bradley et al. (2010)
~0.08	$\mathrm{h^{-1}}$	$(24 \cdot \chi^C / r^{C:N})$ h $\mathrm{day^{-1}}$	Phytoplankton (<35 µm, NH_4)	Bradley et al. (2010)
~0.016	$\mathrm{h^{-1}}$	$(24 \cdot \chi^C / r^{C:N})$ h $\mathrm{day^{-1}}$	Phytoplankton (<35 µm, NO_3)	Bradley et al. (2010)
~0.04–0.07	$\mathrm{h^{-1}}$	$(24 \cdot \chi^C / r^{C:N})$ h $\mathrm{day^{-1}}$	Phytoplankton (eutrophic, subtropical lake, NH_4)	Gu et al. (1997)
~0.02	$\mathrm{h^{-1}}$	$(24 \cdot \chi^C / r^{C:N})$ h $\mathrm{day^{-1}}$	Phytoplankton (eutrophic, subtropical lake, NO_3)	Gu et al. (1997)
~0.3–0.85	$\mathrm{mol(NO_3)\,(mol(C)\,day)^{-1}}$	χ^C $\mathrm{fmol(C)\,cell^{-1}}$	Diatoms (NO_3)	Litchman et al. (2007)
~0.05–0.1	$\mathrm{mol(NO_3)\,(mol(C)\,day)^{-1}}$	χ^C $\mathrm{fmol(C)\,cell^{-1}}$	Coccolithophorids (NO_3)	Litchman et al. (2007)
~0.001–0.1	$\mathrm{mol(NO_3)\,(mol(C)\,day)^{-1}}$	χ^C $\mathrm{fmol(C)\,cell^{-1}}$	Dinoflagellates (NO_3)	Litchman et al. (2007)
~0.15	$\mathrm{mol(NO_3)\,(mol(C)\,day)^{-1}}$	χ^C $\mathrm{fmol(C)\,cell^{-1}}$	Green algae (NO_3)	Litchman et al. (2007)
~0.08	$\mathrm{h^{-1}}$	$(24 \cdot \chi^C / r^{C:N})$ h $\mathrm{day^{-1}}$	Bacteria (0.2–0.8 µm, NH_4)	Bradley et al. (2010)
~0.006	$\mathrm{h^{-1}}$	$(24 \cdot \chi^C / r^{C:N})$ h $\mathrm{day^{-1}}$	Bacteria (0.2–0.8 µm, NO_3)	Bradley et al. (2010)

Table S12. DIN uptake half saturation constants K_N.

Range	Unit	Note	Source
<0.5	$\mu M(N)$	Oceanic phytoplankton (oligotrophic)	Laws (2013)
>1.0	$\mu M(N)$	Coastal phytoplankton (eutrophic)	Laws (2013)
2.24–8.71	$\mu M(N)$	Phytoplankton (eutrophic, subtropical lake, NH_4)	Gu et al. (1997)
2.21	$\mu M(N)$	Phytoplankton (eutrophic, subtropical lake, NO_3)	Gu et al. (1997)
~0.2–2.5	$\mu M(NO_3)$	Diatoms (NO_3)	Litchman et al. (2007)
~0.01–0.02	$\mu M(NO_3)$	Coccolithophorids (NO_3)	Litchman et al. (2007)
~2.0–9.5	$\mu M(NO_3)$	Dinoflagellates (NO_3)	Litchman et al. (2007)
~0.03–6.3	$\mu M(NO_3)$	Green algae (NO_3)	Litchman et al. (2007)
1.6 ± 1.9	$\mu M(N)$	Diatoms	Sarthou et al. (2005)

S7.3 Organic Matter Uptake Parameters

Heterotrophic uptake of dissolved organic matter (DOM) is governed by maximum uptake rates (V_{DOC}, V_{DON}), half-saturation constants (K_{DOC}, K_{DON}), and biomass yield coefficients (Y_{DOC}, Y_{DON}). These parameters vary substantially across substrates, bacterial groups, and environmental conditions (Tables S13–S15). Reported V_{DOC} values span four orders of magnitude, reflecting substrate specificity and adaptation strategies (Kovarova and Egli, 1998). Half-saturation constants K_{DOC} range from nM to mM carbon equivalents, typically lower in oligotrophic systems. Note that V_{DOC} and K_{DOC} are often correlated, such that the specific affinity (V_{DOC}/K_{DOC}) exhibits less variability (Behrenfeld et al., 2004).

We don't list DON parameters separately. For nitrogen-containing compounds, parameters can be derived using the compound's elemental composition. Carbon-based specific rates have to be converted to cell-specific units using cellular carbon content. Importantly, most available data derives from single-substrate experiments; community-level kinetics in bulk DOM pools may differ due to parallel uptake pathways (Mentges et al., 2019). On a theoretical basis, one may argue that for uptake of a bulk of compounds, the half-saturation constants should be assumed higher than for the uptake of an individual compound dependent on the diversity of compound constituting the bulk (see Appendix S7.5).

Crucially, the yield coefficient Y_{DOC} differs from bacterial growth efficiency (BGE), although BGE is an important source to estimate appropriate values. BGE measures biomass carbon production per DOC uptake (del Giorgio and Cole, 1998), while in MCoM $1 - Y_{DOC}$ exclusively represents the metabolic costs of biomass synthesis. In MCoM, continuous population losses [Eqn. (9) of the main text] account for maintenance, leakage, senescence, and other mortality factors, and are not included for the yield. However, these processes decrease the BGE with a degree dependent on the specific measurement protocol. Thus BGE $\leq Y_{DOC}$. We recommend approximating Y_{DOC} by maximal observed BGE for the substrate. For nitrogen, $Y_{DON} > Y_{DOC}$ is expected. For instance, amino acids show higher incorporation efficiency than sugars (del Giorgio and Cole, 1998).

When converting dry weight to biomass carbon, the carbon fraction w_C of dry weight, has to be known or assumed. This varies by taxon and environmental conditions. For instance, Fagerbakke et al. (1996) report 30–60% for heterotrophic bacteria. Likewise, when biovolume measurements are used, it is important to consider that cell carbon density varies considerably (12–605 $\mathrm{fg(C)\,\mu m^{-3}}$; Vrede et al. (2002)). For phytoplankton, $w_C = 0.5$ has been used for *Prochlorococcus* (Bertilsson et al., 2003), $w_C = 0.35$ for diatoms, and $w_C = 0.45$ for other eukaryotic microalgae (Finkel et al., 2016).

Table S13. Maximal rates V_{DOC} for heterotrophic DOC uptake.

Range	Unit	Conversion to model unit $(\mathrm{fmol(C)\,(cell\,day)^{-1}})$	Note	Source
0.36–0.65	$\mathrm{fg(C)\,(cell\cdot h)^{-1}}$	$2\ \frac{\mathrm{fmol\,h}}{\mathrm{fg\,day}}$	Free-living marine (on glucose)	Azúa and Unanue (2007)
2.71–26.28	$\mathrm{fg(C)\,(cell\cdot h)^{-1}}$	$2\ \frac{\mathrm{fmol\,h}}{\mathrm{fg\,day}}$	Aggregate-associated (on glucose)	Azúa and Unanue (2007)
0.35–0.45	$\mathrm{fg(C)\,(cell\cdot h)^{-1}}$	$2\ \frac{\mathrm{fmol\,h}}{\mathrm{fg\,day}}$	Free-living marine (on leucine)	Azúa and Unanue (2007)
0.65–9.05	$\mathrm{fg(C)\,(cell\cdot h)^{-1}}$	$2\ \frac{\mathrm{fmol\,h}}{\mathrm{fg\,day}}$	Aggregate-associated (on leucine)	Azúa and Unanue (2007)
1.2	$\mathrm{\mu g(tol)\,(mg(CDW)\,h)^{-1}}$	$2.20\cdot10^{-2}\cdot\chi^C/w_C\ \frac{\mathrm{fmol(C)\,mg(CDW)\,h}}{\mathrm{mg(tol)\,cells\,day}}$ †	Marine bacterium (on toluene)	Button (1998)
0.13	$\mathrm{\mu g(ace)\,(mg(CDW)\,h)^{-1}}$	$0.96\cdot10^{-2}\cdot\chi^C/w_C\ \frac{\mathrm{fmol(C)\,mg(CDW)\,h}}{\mathrm{mg(tol)\,cells\,day}}$ †	Marine bacterium (on acetate)	Button (1998)
0.23–110	$\mathrm{nmol(glu)\,(min\cdot mg(CDW))^{-1}}$	$0.104\cdot\chi^C/w_C\ \frac{\mathrm{fmol(C)\,mg(CDW)\,min}}{\mathrm{nmol(glu)\,cells\,day}}$ ‡	Marine cultures (on glucose)	Schut et al. (1993)
0.7–124	$\mathrm{nmol(glt)\,(min\cdot mg(CDW))^{-1}}$	$0.086\cdot\chi^C/w_C\ \frac{\mathrm{fmol(C)\,mg(CDW)\,min}}{\mathrm{nmol(glu)\,cells\,day}}$ ‡	Marine cultures (on glutamate)	Schut et al. (1993)

†: Assuming carbon to constitute w_C percent of the cell dry weight (CDW), one $\mathrm{mg(CDW)}$ has a molar carbon content of $10^{12}\cdot w_C/12\ \mathrm{fmol(C)\ mg(CDW)^{-1}}$. In cell numbers this gives $10^{12}\cdot(w_C/12)\cdot(\chi^C)^{-1}\ \mathrm{cells/mg(CDW)}$. Further, carbon constitutes 91.3% of the weight of toluene (C_7H_8), giving $(0.913/12)$ $(\mathrm{\mu mol(C)\,\mu g(tol)^{-1}})$ $= (0.913/12)\cdot10^9\ \mathrm{(fmol(C)\,\mu g(tol)^{-1})}$. Additionally accounting for conversion the rate from $\mathrm{h^{-1}}$ to $\mathrm{d^{-1}}$ yields the tabulated conversion factor. For acetate ($C_2H_3O_2$), the conversion is analogous, with 40.1% of its weight constituted by carbon.

‡: Using a molar carbon content $(6\cdot10^6\ \mathrm{fmol(C)/nmol(glu)}$ of glucose, $(6\cdot10^6\ \mathrm{fmol(C)/nmol(glu)}$ of glucose ($C_6H_{12}O_6$), $(6\cdot10^6\ \mathrm{fmol(C)/nmol(glu)}$ of glutamate ($C_5H_9NO_4$), $24\cdot60\ \mathrm{min/day}$, and the conversion of mg(CDW) to cell number (see †). Using the cell weight estimate above we obtain a total conversion factor of $0.052\cdot\chi^C$ for glucose, and $0.043\cdot\chi^C$ for glutamate.

Table S14. Half saturation constants K_{DOC} for heterotrophic organic matter assimilation.

Range	Unit	Conversion to model unit	Note	Source
2.62–13.62	$\mathrm{\mu g(C)\,L^{-1}}$	$(1/12)$ $\mathrm{\mu mol(C)\,\mu g(C)}$	Free-living marine (on glucose)	Azúa and Unanue (2007)
101.1–131.0	$\mathrm{\mu g(C)\,L^{-1}}$	$(1/12)$ $\mathrm{\mu mol(C)\,\mu g(C)}$	Aggregate-associated (on glucose)	Azúa and Unanue (2007)
1.18–1.70	$\mathrm{\mu g(C)\,L^{-1}}$	$(1/12)$ $\mathrm{\mu mol(C)\,\mu g(C)}$	Free-living marine (on leucine)	Azúa and Unanue (2007)
5.28–41.08	$\mathrm{\mu g(C)\,L^{-1}}$	$(1/12)$ $\mathrm{\mu mol(C)\,\mu g(C)}$	Aggregate-associated (on leucine)	Azúa and Unanue (2007)
10.0	$\mathrm{\mu g(tol)\,L^{-1}}$	0.076 $\mathrm{\mu mol(C)\,\mu g(tol)}$ †	Marine bacterium (on toluene)	Button (1998)
20000	$\mathrm{\mu g(ace)\,L^{-1}}$	0.033 $\mathrm{\mu mol(C)\,\mu g(ace)}$ †	Marine bacterium (on acetate)	Button (1998)
2.3–590000	$\mathrm{nM(glu)}$	$6\cdot10^{-3}$ $\mathrm{\mu mol(C)\,nmol(glu)^{-1}}$	Marine cultures (on glucose)	Schut et al. (1993)
18-911	$\mathrm{nM(glt)}$	$5\cdot10^{-3}$ $\mathrm{\mu mol(C)\,nmol(glt)^{-1}}$	Marine cultures (on glutamate)	Schut et al. (1993)
0.6–255	$\mathrm{nM(substrate)}$	$(4-6)\cdot10^{-3}$ $\mathrm{\mu mol(C)\,nmol(s.)^{-1}}$ ‡	Natural assemblage (low conc.)	Casey et al. (2015)
54.2–368.3	$\mathrm{nM(substrate)}$	$(4-6)\cdot10^{-3}$ $\mathrm{\mu mol(C)\,nmol(s.)^{-1}}$ ‡	Natural assemblage (high conc.)	Casey et al. (2015)

†: see notes below Table S13.

‡: Cultures on simple substrates with 4–6 carbon atoms and 0–4 nitrogen atoms.

Table S15. Kinetic parameters for heterotrophic organic matter assimilation.

Range	Unit	Conversion to model unit	Note	Source
Y_{DOC}	0.81	–	Max marine BGE (phytoplankton exudates)	del Giorgio and Cole (1998)
Y_{DOC}	0.91	–	Max freshwater BGE (plant detritus)	del Giorgio and Cole (1998)
Y_{DON}	$\geq Y_{DOC}$	–	e.g., amino acids $\geq$ sugars	del Giorgio and Cole (1998)

S7.4 Photosynthesis Parameters

Photosynthetic parameters exhibit wide variation across phytoplankton groups and environmental conditions (Enríquez et al., 1996). Chlorophyll-a normalized rates and carbon-to-chlorophyll ratios are influenced by temperature, nutrient availability, and light adaptation, requiring careful parametrization for different ecological contexts. In MCoM, the photosynthesis rate can either be set directly through environment.irradiance when variant.use_PI_curve=false, or it can be parametrized as a response to the environmental irradiance (PI-curve). The shape of the PI-curve is defined by the light-saturated photosynthesis rate $\overline{\phi}$ ($\mathrm{mol(C)\,mol(Chl)^{-1}\,day^{-1}}$), its initial slope α ($\frac{\mathrm{mol(C)\,m^2\,s}}{\mathrm{mol(chl)\,day\,\mu mol(Q)}}$), and the photo inhibition coefficient β ($\frac{\mathrm{mol(C)\,m^2\,s}}{\mathrm{mol(chl)\,day\,\mu mol(Q)}}$). Tables S16 and S17 summarize reported ranges for these parameters.

Carbon-to-chlorophyll ratios ($r^{C:Chl}$) generally decrease with increasing light levels and growth rates (Geider, 1987; Langdon, 1988). At constant light levels, values for $r^{C:Chl}$ decrease with increasing temperature (Geider, 1987). Nutrient-limitation can induce elevated $r^{C:Chl}$ (Geider, 1987; Riemann et al., 1989). For dinoflagellates and cyanobacteria, higher $r^{C:Chl}$ have been reported compared to diatoms and green algae under comparable conditions. As a consequence, dinoflagellates generally have a lower light-saturated photosynthesis rate $\overline{\phi}$ (Geider, 1987; Lacour et al., 2017). Further, $\overline{\phi}$ is strongly influenced by temperature with higher rates at higher temperatures (Edwards et al., 2016; Lacour et al., 2017). The initial Slope of the PI-Curve (α) exhibits significant covariation with $\overline{\phi}$, manifest in a reduced variation of the light saturation index $\overline{\phi}/\alpha$ (Behrenfeld et al., 2004). As the light-saturated photosynthetic rate, α is strongly correlated with temperature (Côté and Platt, 1983).

Table S16. Reported ranges for carbon-to-chlorophyll ratios $r^{C:Chla}$.

Range	Unit	Conversion to model unit† $(\mathrm{mol(C)\,mol(chl)^{-1}})$	Note	Source
91–105	$\mathrm{g(C)\,g(chl)^{-1}}$	$74.33\ \frac{\mathrm{mol(C)\,g(chl)}}{\mathrm{g(C)\,mol(chl)}}$	Natural assemblage, surface (nutrient-poor), California	Eppley (1968)
22–28	$\mathrm{g(C)\,g(chl)^{-1}}$	$74.33\ \frac{\mathrm{mol(C)\,g(chl)}}{\mathrm{g(C)\,mol(chl)}}$	Natural assemblage, deeper (nutrient-rich), California	Eppley (1968)
~6–40	$\mathrm{g(C)\,g(chl)^{-1}}$	$74.33\ \frac{\mathrm{mol(C)\,g(chl)}}{\mathrm{g(C)\,mol(chl)}}$	Diatoms (decreasing C:Chl-a with temperature)	Geider (1987)
50.4–204.6	$\mathrm{g(C)\,g(chl)^{-1}}$	$74.33\ \frac{\mathrm{mol(C)\,g(chl)}}{\mathrm{g(C)\,mol(chl)}}$	Synechococcus at different irradiances	Kana and Glibert (1987)
15.6–27.0	$\mathrm{g(C)\,g(chl)^{-1}}$	$74.33\ \frac{\mathrm{mol(C)\,g(chl)}}{\mathrm{g(C)\,mol(chl)}}$	Diatoms	Langdon (1988)
11.4–13.3	$\mathrm{g(C)\,g(chl)^{-1}}$	$74.33\ \frac{\mathrm{mol(C)\,g(chl)}}{\mathrm{g(C)\,mol(chl)}}$	Chlorophytes	Langdon (1988)
52.6–77.0	$\mathrm{g(C)\,g(chl)^{-1}}$	$74.33\ \frac{\mathrm{mol(C)\,g(chl)}}{\mathrm{g(C)\,mol(chl)}}$	Dinoflagellates	Langdon (1988)
0.72–3.05	% of total carbon	$55.01\ \frac{\mathrm{mol(C)\,g(C,chl)}}{\mathrm{g(C)\,mol(chl)}}$	Phytoplankton batch cultures, nutrient-poor	Riemann et al. (1989)
1.22–6.08	% of total carbon	$55.01\ \frac{\mathrm{mol(C)\,g(C,chl)}}{\mathrm{g(C)\,mol(chl)}}$	Phytoplankton batch cultures, nutrient-replete	Riemann et al. (1989)
28.28 ± 11.84	$\mathrm{g(C)\,g(chl)^{-1}}$	$74.33\ \frac{\mathrm{mol(C)\,g(chl)}}{\mathrm{g(C)\,mol(chl)}}$	Polar diatoms	Lacour et al. (2017)
24.47 ± 8.34	$\mathrm{g(C)\,g(chl)^{-1}}$	$74.33\ \frac{\mathrm{mol(C)\,g(chl)}}{\mathrm{g(C)\,mol(chl)}}$	Temperate diatoms	Lacour et al. (2017)

†: Using the molar weight of chlorophyll-a ($1\ \mathrm{mol(chl)} = 892\ \mathrm{g(chl)}$), with carbon responsible for 74% of the weight ($1\ \mathrm{g(chl)} = 0.74\ \mathrm{g(C,chl)}$), we obtain the tabulated conversion factors to molar ratios. Note that the model is parametrized by $r^{Chla:C} = (r^{C:Chla})^{-1}$, i.e., by the inverted value obtained with the tabulated factor.

Table S17. Reported ranges for PI-curve parameters $\overline{\phi}$, α, and β.

Parameter	Range	Unit	Conversion to model unit† $\left(\frac{\mathrm{mol(C)\,m^2\,s}}{\mathrm{mol(chl)\,day\,\mu mol(Q)}}\right)$	Note	Source
α	0.038–0.95	$\frac{\mathrm{mg(C)\,m^2}}{\mathrm{mg(chl)\,h\,W}}$	$\vartheta_\phi/\vartheta_{W\to I}$	Eukaryotic phytoplankton (mainly diatoms)	Platt et al. (1980)
α	~0.01–0.30	$\frac{\mathrm{mg(C)\,m^2\,s}}{\mathrm{mg(chl)\,h\,\mu mol(Q)}}$	ϑ_ϕ	Natural phytoplankton assemblage (California coast)	Harding et al. (1982)
α	~0.07–0.26	$\frac{\mathrm{mg(C)\,m^2}}{\mathrm{mg(chl)\,h\,W}}$	$\vartheta_\phi/\vartheta_{W\to I}$	Natural phytoplankton assemblage (North West Atlantic)	Côté and Platt (1983)
α	~0.01–0.11	$\frac{\mathrm{mg(C)\,m^2\,s}}{\mathrm{mg(chl)\,h\,\mu mol(Q)}}$	ϑ_ϕ	Natural phytoplankton assemblage (North East Pacific)	Forbes et al. (1986)
α	0.12–0.129	$\frac{\mathrm{mg(C)\,m^2\,s}}{\mathrm{mg(chl)\,h\,\mu mol(Q)}}$	ϑ_ϕ	PE-containing cyanobacteria	Langdon (1988)
α	0.013–0.087 (avg. 0.021)	$\frac{\mathrm{mg(C)\,m^2\,s}}{\mathrm{mg(chl)\,h\,\mu mol(Q)}}$	ϑ_ϕ	Compilation of different diatoms	Sarthou et al. (2005)
			$\left(\frac{\mathrm{mol(C)\,m^2\,s}}{\mathrm{mol(chl)\,day\,\mu mol(Q)}}\right)$		
β	0.0–0.011	$\frac{\mathrm{mg(C)\,m^2\,s}}{\mathrm{mg(chl)\,h\,\mu mol(Q)}}$	ϑ_ϕ	Eukaryotic phytoplankton (mainly diatoms)	Platt et al. (1980)
			$(\mathrm{mol(C)\,(mol(chl)\,day)^{-1}})$		
$\overline{\phi}$	~0.5–20	$\mathrm{mg(C)\,(mg(chl)\,h)^{-1}}$	ϑ_ϕ	Eukaryotic phytoplankton (mainly diatoms)	Platt et al. (1980)
$\overline{\phi}$	~0.5–24.3	$\mathrm{mg(C)\,(mg(chl)\,h)^{-1}}$	ϑ_ϕ	Natural phytoplankton assemblage (California coast)	Harding et al. (1982)
$\overline{\phi}$	~2.3–8.2	$\mathrm{mg(C)\,(mg(chl)\,h)^{-1}}$	ϑ_ϕ	Natural phytoplankton assemblage (North West Atlantic)	Côté and Platt (1983)
$\overline{\phi}$	~1.0–17.2	$\mathrm{mg(C)\,(mg(chl)\,h)^{-1}}$	ϑ_ϕ	Natural phytoplankton assemblage (North East Pacific)	Forbes et al. (1986)
$\overline{\phi}$	1.2–11.4 (avg. 2.6)	$\mathrm{mg(C)\,(mg(chl)\,h)^{-1}}$	ϑ_ϕ	Diatoms, smaller $\overline{\phi}$ for polar species	Sarthou et al. (2005)

†: To convert irradiance values from energy flux density ($\mathrm{W\,m^{-2}}$) to flux density of photosynthetically active radiation ($\mu\mathrm{mol\,(m^2\,s)^{-1}}$), the conversion factor $\vartheta_{W\to I}$ depends on the distribution of wavelengths. Commonly used values are $\vartheta_{W\to I} = 4.15$ to $5.0\ \mu\mathrm{mol(Q)\,(W\,s)^{-1}}$ (Geider, 1987; Enríquez et al., 1996).
The factor $\vartheta_\phi = 1784\ \frac{\mathrm{mol(C)\,mg(chl)\,h}}{\mathrm{mg(C)\,mol(chl)\,day}}$ is used to convert chlorophyll-specific, hourly photosynthesis rates in to daily molar rates used in MCoM, cf. note below Table S16.

S7.5 Kinetic parameters for bulk DOM representations

Bulk DOM pool representations in MCoM require careful consideration of effective parameters. Let us assume a population H consumes a single DOC type D_0 with kinetic parameters V_0 and K_0. That is, the maximal DOC uptake rate for H is

$$f_{\mathrm{DOC}}^{\max} = \frac{V_0 \cdot D_0}{K_0 + D_0}$$

In natural environments, heterotrophic bacteria feed simultaneously on a multitude of different organic compounds (Kovarova and Egli, 1998; Zakem et al., 2021). In models, these compounds are often represented by one or several pools representing the entire bulk DOC or different groups of organic compounds (Mentges et al., 2019; Marsland et al., 2020). Let us consider that D_0 represents such a pool of ten different compounds $D_1, ..., D_{10}$, which are metabolically independent, i.e.,

$$f_{\mathrm{DOC}}^{\max} = \sum_{i=1}^{10} \frac{V_i \cdot D_i}{K_i + D_i}.$$

For simplicity, we further assume that all individual compounds have identical concentrations ($D_i = D_0/10$) and identical half saturation constants K_i. Since the total maximal uptake corresponds to the metabolic capacity, it seems reasonable to assume $\sum_i V_i = V_0$. This implies,

$$\frac{V_0 \cdot D_0}{K_0 + D_0} = \sum_{i=1}^{10} \frac{V_i \cdot D_i}{K_i + D_i} = \frac{V_0 \cdot D_0/10}{K_i + D_0/10} = \frac{V_0 \cdot D_0}{10 \cdot K_i + D_0}$$

Hence, $K_i \equiv K_0/10$.

This is a (very rough) argument, which illustrates that the half saturation constant K_0 for the bulk pool has to be assumed larger than the constants K_i of the individual pools. If the assumptions that we made here approximately hold, one may estimate

$$K_{\text{bulk}} = \{\text{no. compounds}\} \times K_{\text{individual}}$$

S8 Integration scheme

Starting from a given initial state $\boldsymbol{X}_0 = (\boldsymbol{P}_0, \boldsymbol{H}_0, \boldsymbol{D}_0, \boldsymbol{M}_0, N_0)$, MCoM generates trajectories using an Adams-Bashforth explicit two-step method (Butcher, 2005). This method generates state approximations at equidistant time points $t_n = t_0 + n \cdot dt$ using the formula

$$\boldsymbol{X}_{n+2} = \boldsymbol{X}_{n+1} + \left[\frac{3}{2} f\left(t_{n+1}, \boldsymbol{X}_{n+1}\right) - \frac{1}{2} f\left(t_n, \boldsymbol{X}_n\right)\right] dt, \tag{S5}$$

where $\boldsymbol{X}_n$ is the vector containing the system state at time t_n.

References

Azúa, I. and Unanue, M.: Influence of Age of Aggregates and Prokaryotic Abundance on Glucose and Leucine Uptake by Heterotrophic Marine Prokaryotes, International Microbiology, pp. 13–18, https://doi.org/10.2436/20.1501.01.3, 2007.

Behrenfeld, M. J., Prasil, O., Babin, M., and Bruyant, F.: IN SEARCH OF A PHYSIOLOGICAL BASIS FOR COVARIATIONS IN LIGHT-LIMITED AND LIGHT-SATURATED PHOTOSYNTHESIS[1], Journal of Phycology, 40, 4–25, https://doi.org/10.1046/j.1529-8817.2004.03083.x, 2004.

Bertilsson, S., Berglund, O., Karl, D. M., and Chisholm, S. W.: Elemental Composition of Marine *Prochlorococcus* and *Synechococcus* : Implications for the Ecological Stoichiometry of the Sea, Limnology and Oceanography, 48, 1721–1731, https://doi.org/10.4319/lo.2003.48.5.1721, 2003.

Bradley, P., Sanderson, M., Nejstgaard, J., Sazhin, A., Frischer, M., Killberg-Thoreson, L., Verity, P., Campbell, L., and Bronk, D.: Nitrogen Uptake by Phytoplankton and Bacteria during an Induced Phaeocystis Pouchetii Bloom, Measured Using Size Fractionation and Flow Cytometric Sorting, Aquatic Microbial Ecology, 61, 89–104, https://doi.org/10.3354/ame01414, 2010.

Butcher, J. C., ed.: Numerical Methods for Ordinary Differential Equations, Wiley, Chichester, ISBN 978-0-471-96758-3 978-0-470-86827-0, https://doi.org/10.1002/0470868279, 2005.

Button, D. K.: Nutrient Uptake by Microorganisms According to Kinetic Parameters from Theory as Related to Cytoarchitecture, Microbiology and Molecular Biology Reviews, 62, 636–645, https://doi.org/10.1128/MMBR.62.3.636-645.1998, 1998.

Casey, J. R., Falkowski, P. G., and Karl, D. M.: Substrate Selection for Heterotrophic Bacterial Growth in the Sea, Marine Chemistry, 177, 349–356, https://doi.org/10.1016/j.marchem.2015.06.032, 2015.

Christie-Oleza, J. A., Sousoni, D., Lloyd, M., Armengaud, J., and Scanlan, D. J.: Nutrient Recycling Facilitates Long-Term Stability of Marine Microbial Phototroph–Heterotroph Interactions, Nature Microbiology, 2, 17 100, https://doi.org/10.1038/nmicrobiol.2017.100, 2017.

Côté, B. and Platt, T.: Day-to-day variations in the spring-summer photosynthetic parameters of coastal marine phytoplankton, Limnology and Oceanography, 28, 320–344, 1983.

del Giorgio, P. A. and Cole, J. J.: BACTERIAL GROWTH EFFICIENCY IN NATURAL AQUATIC SYSTEMS, Annual Review of Ecology and Systematics, 29, 503–541, https://doi.org/10.1146/annurev.ecolsys.29.1.503, 1998.

Edwards, K. F., Thomas, M. K., Klausmeier, C. A., and Litchman, E.: Phytoplankton Growth and the Interaction of Light and Temperature: A Synthesis at the Species and Community Level, Limnology and Oceanography, 61, 1232–1244, https://doi.org/10.1002/lno.10282, 2016.

Enríquez, S., Duarte, C. M., Sand-Jensen, K., and Nielsen, S. L.: Broad-Scale Comparison of Photosynthetic Rates across Phototrophic Organisms, Oecologia, 108, 197–206, https://doi.org/10.1007/BF00334642, 1996.

Eppley, R. W.: AN INCUBATION METHOD FOR ESTIMATING THE CARBON CONTENT OF PHYTOPLANKTON IN NATURAL SAMPLES1, Limnology and Oceanography, 13, 574–582, https://doi.org/10.4319/lo.1968.13.4.0574, 1968.

Fagerbakke, K. M., Heldal, M., and Norland, S.: Content of Carbon, Nitrogen, Oxygen, Sulfur and Phosphorus in Native Aquatic and Cultured Bacteria, Aquatic Microbial Ecology, 10, 15–27, 1996.

Finkel, Z. V., Follows, M. J., and Irwin, A. J.: Size-Scaling of Macromolecules and Chemical Energy Content in the Eukaryotic Microalgae, Journal of Plankton Research, 38, 1151–1162, https://doi.org/10.1093/plankt/fbw057, 2016.

Forbes, J., Denman, K., and Mackas, D.: Determination of photosynthetic capacity in coastal marine phytoplankton: Effects of assay irradiance and variability of photosynthetic parameters, Marine Ecology Progress Series, 32, 181–191, 1986.

Fukuda, R., Ogawa, H., Nagata, T., and Koike, I.: Direct Determination of Carbon and Nitrogen Contents of Natural Bacterial Assemblages in Marine Environments, Applied and Environmental Microbiology, 64, 3352–3358, https://doi.org/10.1128/AEM.64.9.3352-3358.1998, 1998.

Geider, R. and La Roche, J.: Redfield Revisited: Variability of C:N:P in Marine Microalgae and Its Biochemical Basis, European Journal of Phycology, 37, 1–17, https://doi.org/10.1017/S0967026201003456, 2002.

Geider, R. J.: Light and Temperature Dependence of the Carbon to Chlorophyll a Ratio in Microalgae and Cyanobacteria: Implications for Physiology and Growth of Phytoplankton, The New Phytologist, 106, 1–34, 1987.

Godwin, C. M. and Cotner, J. B.: Stoichiometric flexibility in diverse aquatic heterotrophic bacteria is coupled to differences in cellular phosphorus quotas, Frontiers in Microbiology, 6, https://doi.org/10.3389/fmicb.2015.00159, 2015.

Goldman, J. C., McCarthy, J. J., and Peavey, D. G.: Growth Rate Influence on the Chemical Composition of Phytoplankton in Oceanic Waters, Nature, 279, 210–215, https://doi.org/10.1038/279210a0, 1979.

Grob, C., Ostrowski, M., Holland, R. J., Heldal, M., Norland, S., Erichsen, E. S., Blindauer, C., Martin, A. P., Zubkov, M. V., and Scanlan, D. J.: Elemental Composition of Natural Populations of Key Microbial Groups in A Tlantic Waters, Environmental Microbiology, 15, 3054–3064, https://doi.org/10.1111/1462-2920.12145, 2013.

Gu, B., Havens, K. E., Schelske, C. L., and Rosen, B. H.: Uptake of Dissolved Nitrogen by Phytoplankton in a Eutrophic Subtropical Lake, Journal of Plankton Research, 19, 759–770, https://doi.org/10.1093/plankt/19.6.759, 1997.

Harding, L. W., Prézelin, B. B., Sweeney, B. M., and Cox, J. L.: Diel Oscillations of the Photosynthesis-Irradiance (P-I) Relationship in Natural Assemblages of Phytoplankton, Marine Biology, 67, 167–178, https://doi.org/10.1007/BF00401282, 1982.

Kana, T. M. and Glibert, P. M.: Effect of Irradiances up to 2000 μE M-2 S-1 on Marine Synechococcus WH7803—I. Growth, Pigmentation, and Cell Composition, Deep Sea Research Part A. Oceanographic Research Papers, 34, 479–495, https://doi.org/10.1016/0198-0149(87)90001-X, 1987.

Kirchman, D. L.: The Uptake of Inorganic Nutrients by Heterotrophic Bacteria, Microbial Ecology, 28, 255–271, https://doi.org/10.1007/BF00166816, 1994.

Kovarova, K. and Egli, T.: Growth Kinetics of Suspended Microbial Cells: From Single-Substrate-Controlled Growth to Mixed-Substrate Kinetics, Microbiology and Molecular Biology Reviews, 62, 646–666, 1998.

Kroer, N., Jørgensen, N. O. G., and Coffin, R. B.: Utilization of Dissolved Nitrogen by Heterotrophic Bacterioplankton: A Comparison of Three Ecosystems, Applied and Environmental Microbiology, 60, 4116–4123, https://doi.org/10.1128/aem.60.11.4116-4123.1994, 1994.

Lacour, T., Larivière, J., and Babin, M.: Growth, Chl *a* Content, Photosynthesis, and Elemental Composition in Polar and Temperate Microalgae, Limnology and Oceanography, 62, 43–58, https://doi.org/10.1002/lno.10369, 2017.

Langdon, C.: On the Causes of Interspecific Differences in the Growth-Irradiance Relationship for Phytoplankton. II. A General Review, Journal of Plankton Research, 10, 1291–1312, https://doi.org/10.1093/plankt/10.6.1291, 1988.

Laws, E. A.: Evaluation of In Situ Phytoplankton Growth Rates: A Synthesis of Data from Varied Approaches, Annual Review of Marine Science, 5, 247–268, https://doi.org/10.1146/annurev-marine-121211-172258, 2013.

Litchman, E., Klausmeier, C. A., Schofield, O. M., and Falkowski, P. G.: The Role of Functional Traits and Trade-Offs in Structuring Phytoplankton Communities: Scaling from Cellular to Ecosystem Level, Ecology Letters, 10, 1170–1181, https://doi.org/10.1111/j.1461-0248.2007.01117.x, 2007.

Marsland, R., Cui, W., and Mehta, P.: A Minimal Model for Microbial Biodiversity Can Reproduce Experimentally Observed Ecological Patterns, Scientific Reports, 10, 3308, https://doi.org/10.1038/s41598-020-60130-2, 2020.

Mentges, A., Feenders, C., Deutsch, C., Blasius, B., and Dittmar, T.: Long-Term Stability of Marine Dissolved Organic Carbon Emerges from a Neutral Network of Compounds and Microbes, Scientific Reports, 9, 17 780, https://doi.org/10.1038/s41598-019-54290-z, 2019.

Platt, T., Gallegos, C. L., and Harrison, W. G.: Photoinhibition of Photosynthesis in Natural Assemblages of Marine Phytoplankton, Journal of Marine Research, 38, 1980.

Redfield, A. C.: The biological control of chemical factors in the environment, American scientist, 46, 230A–221, 1958.

Riemann, B., Simonsen, P., and Stensgaard, L.: The Carbon and Chlorophyll Content of Phytoplankton from Various Nutrient Regimes, Journal of Plankton Research, 11, 1037–1045, https://doi.org/10.1093/plankt/11.5.1037, 1989.

Sarthou, G., Timmermans, K. R., Blain, S., and Tréguer, P.: Growth Physiology and Fate of Diatoms in the Ocean: A Review, Journal of Sea Research, 53, 25–42, https://doi.org/10.1016/j.seares.2004.01.007, 2005.

Schut, F., De Vries, E. J., Gottschal, J. C., Robertson, B. R., Harder, W., Prins, R. A., and Button, D. K.: Isolation of Typical Marine Bacteria by Dilution Culture: Growth, Maintenance, and Characteristics of Isolates under Laboratory Conditions, Applied and Environmental Microbiology, 59, 2150–2160, https://doi.org/10.1128/aem.59.7.2150-2160.1993, 1993.

Sher, D., Thompson, J. W., Kashtan, N., Croal, L., and Chisholm, S. W.: Response of *Prochlorococcus* Ecotypes to Co-Culture with Diverse Marine Bacteria, The ISME Journal, 5, 1125–1132, https://doi.org/10.1038/ismej.2011.1, 2011.

Tas, S.: Estimation of Cellular Carbon Content Based on the Cell Biovolume of Microalgae from a Eutrophic Estuary (Sea of Marmara, Türkiye), Environmental Monitoring and Assessment, 195, 1185, https://doi.org/10.1007/s10661-023-11634-7, 2023.

Vrede, K., Heldal, M., Norland, S., and Bratbak, G.: Elemental Composition (C, N, P) and Cell Volume of Exponentially Growing and Nutrient-Limited Bacterioplankton, Applied and Environmental Microbiology, 68, 2965–2971, https://doi.org/10.1128/AEM.68.6.2965-2971.2002, 2002.

Zakem, E. J., Cael, B. B., and Levine, N. M.: A Unified Theory for Organic Matter Accumulation, Proceedings of the National Academy of Sciences, 118, e2016896 118, https://doi.org/10.1073/pnas.2016896118, 2021.